Material Morphology and Energy Barriers to Electrical Ageing

E.S. Cooper, J.C. Fothergill, L.A. Dissado
Department of Engineering, University of Leicester, Leicester, LE1 7RH, UK

R. N. Hampton*
BICC Cables, Erith, Kent, DA8 1HS, UK

BACKGROUND

Various theories of electro-thermal ageing of high voltage polymeric insulation have been proposed recently, L. A Dissado et al [1], G. Mazzanti et al [2], T. J. Lewis et al [3], J. P. Crine [4], all of which can successfully fit experimental lifetime data, Griffiths et al [5]. However, each model predicts one single time to failure for a set of identical specimens subject to the same electrical field, *E*, and temperature, *T* except as discussed in L. A. Dissado et al [6]. In reality, this is not the case; a distribution of breakdown times is observed. Prediction of this distribution is attempted in this investigation, by a distribution of activation energy parameters within the Dissado-Montanari-Mazzanti (DMM) lifetime model [1], [2]. Investigation of the form of the parameter distributions, and how they change with field and temperature, then gives some insight into the ageing process. The analysis carried out should apply equally well to other lifetime models, since they all contain an activation energy term.

The DMM model predicts a time to failure of polymeric insulation subject to a given electrical stress and temperature as shown below in equation (1).

$$L(E,T) = \frac{\frac{h}{2kT}\exp\left(\frac{-S_d}{k}\right)\exp\left(\frac{H_{dk}-\frac{C_d E^{4b}}{2}}{T}\right)\left(-\ln\left(\frac{A_{eq}(E,T)-A^*}{A_{eq}(E,T)}\right)\right)}{\cosh\left(\frac{K_d - C_d E^{4b}}{2T}\right)}$$

L is predicted lifetime, k is Boltzmann's constant, h is Planck's constant and the C_dE^{4b} term describes the effect of the applied field. The model describes the ageing process in terms of groups of atoms, or moieties within the polymer, undergoing a reversible reaction from a reactant state, to a less energetically favourable product state leading to the initiation of local degradation. This reaction is characterised by an activation energy per moiety, #G, which is made up of an enthalpy part, H_{dk}, and an entropy part, S_d. As a polymer specimen moves towards thermal equilibrium, it moves towards an equilibrium in terms of the number of moieties in each of these states. If the fraction of moieties in the product state, *A*, exceeds a critical fraction, *A** in any localised area, then the insulator is considered to have broken down, since failure in that area becomes inevitable. Catastrophic electrical failure may not yet have occurred, but the insulation can no longer sustain the function for which it was designed.

The DMM model yields one lifetime prediction if all specimens of the same material at a particular temperature and field possess the same values of the governing parameters. Actual experimental results produce a Weibull distribution of lifetimes, J. C. Fothergill and L. A. Dissado [7]. This is because polymers are not homogeneous on an atomic scale, and consequently each of the moieties in a polymeric specimen will have an individual set of parameters describing its own ageing kinetics. The DMM lifetime model contains terms which describe this degradation process, and the values of these are generally obtained by fitting the model to the characteristic lifetime of experimentally obtained lifetime data. However, in each specimen, there will actually be a distribution of physical properties related to ageing, and there must therefore also be a distribution in the model parameters describing the process. Failure will be determined by the most extreme parameter values accessible to a particular specimen [7], so the parameter values obtained by fitting the life expression to the characteristic life will be characteristic values in the extreme value distribution of each parameter.

INVESTIGATION

Extreme value (EV) distributions of activation entropy, S_d, and activation enthalpy, H_{dk}, for the ageing process were investigated, using time to failure data for PET films subject to both AC and DC stress, Gubanski [8]. The AC tests were carried out on films of 50μm thickness, and the DC tests on 36μm films. In the AC case, H_{dk} and S_d distributions were obtained separately; H_{dk} was kept constant while the S_d values were obtained and vice versa. In the DC case S_d was assumed to be zero [2], and only the H_{dk} distribution was investigated.

To investigate the H_{dk} and S_d EV distributions, equation (1) was rearranged in terms of the parameter of interest. This gave an equation in which H_{dk} or S_d was expressed in terms of the other model parameters, *E*, *T* and the time to failure. The other model parameters were assumed to have their characteristic values for PET – calculated using the Levenberg-Marquardt algorithm and published in the literature [2]. For each time to failure datum at a known *E* and *T*, an H_{dk} or an S_d value was calculated. Each value generated in this way was assumed to be the minimum H_{dk} or S_d value for the specimen, mH_{dk} or mS_d. This is reasonable, since the moieties

with the smallest energy barriers age the material quickest, and lead to failure before any of the others, i.e. they are the 'weakest links'. Each lifetime experiment, comprising a set of identical specimens at a certain *E* and *T*, typically tested 9 specimens in the AC case, and 17 in the DC case. The above procedure therefore resulted in a set of 9 mH_{dk} values and mS_d values for each AC test, and 17 mH_{dk} values for each DC test. Since the sets of mH_{dk} and mS_d values were assumed to be minimum values, an approach using extreme value statistics was suitable for their analysis. Reciprocals of mH_{dk} and mS_d were used since an appropriate distribution to model them is the second extreme value distribution $\Lambda_2(z)=\exp(-Z^{\beta})$ with $Z=1/mH_{dk}/\alpha$ or $1/mS_d/\alpha$. This gives the cumulative probability of finding a parameter value greater than Z, i.e. a smaller value of mH_{dk} or mS_d than $1/\alpha$.

The probability density appropriate to this distribution is $Z^{\beta-1}\exp(-Z^{\beta})$, which has the same form as the Weibull function; Weibull graphs can therefore be plotted. When the generated values of $1/mH_{dk}$ and $1/mS_d$ were ranked and plotted in this way, good straight lines were obtained, and these were therefore used to obtain β, the shape parameter, and α the characteristic value of $1/mH_{dk}$ or $1/mS_d$. Values of α and β were calculated for each of the data sets. Large simulated sets data sets of $1/mH_{dk}$ and $1/mS_d$ values were then produced with these α and β characteristics using a Monte Carlo technique. These large distributions were in turn used to generate distributions of lifetime values, using the DMM model and the relevant *E* and *T* values. The generated cumulative probabilities were compared to the original experimental data, and found to be a good fit in both AC and DC cases. Examples are shown in **fig 1.** An investigation was then carried out into the effect of temperature and field on the distributions of $1/mH_{dk}$ and $1/mS_d$. The DMM model assumes that values of H_{dk} and S_d for a given insulation do not change with E or T. It was therefore expected that the characteristic values of the $1/mH_{dk}$ and $1/mS_d$ distributions would be reasonably independent of E and T, but that shape parameters might change.

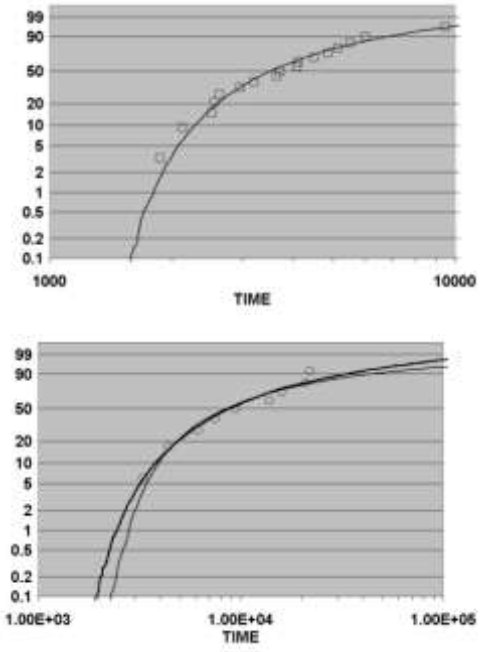

Figure 1 – Weibull cumulative probability with time. Squares are from DC lifetime data, circles from AC lifetime data. Solid lines are from calculated $1/mH_{dk}$ and $1/mS_d$ distributions.

RESULTS

AC results

AC time-to-failure data were available in the range 20°C to 150°C and 10 to 50 kV/mm. Over this range, the $1/mH_{dk}$ and$1/mS_d$ distributions appeared not to be dependent on field. There were, however, various temperature effects. For both the $1/mH_{dk}$ and $1/mS_d$ distributions, the β parameter was found to decrease with increasing temperature. This means that both the distributions became wider with greater temperature. The β parameter was in all cases large ($1.5<\beta<50$ for $1/mH_{dk}$ and $30<\beta<430$ for $1/mS_d$), which means that the distributions of minimum activation energies were all sharp. The α parameter in both distributions appeared to remain independent of temperature until it reached between 60°C and 110°C, a range encompassing the glass transition temperature, T_g, of PET. $1/\alpha$ then began to fall with increasing temperature, L.A. Dissado [9]. Plots of the Weibull parameters with temperature are shown for the AC $1/mH_{dk}$ distributions in **figures 2a and 2b**.

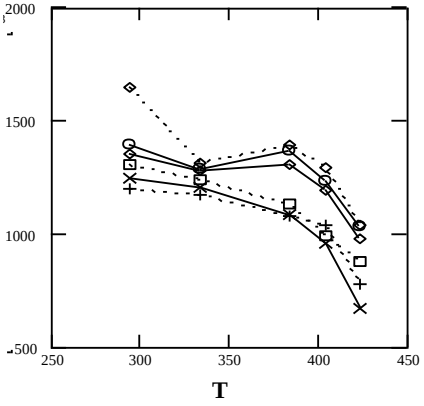

Figure 2a – calculated characteristic mH_{dk} values with temperature for various field strengths.

DC results

DC lifetime data were available in the range 28 to 83kV/mm and from 109°C to 180°C, which is probably above the Tg of PET. As in the AC case, field strength had no effect on either of the Weibull parameters of the $1/mH_{dk}$ distribution. The values of β in the DC case are even greater than in the AC case ($40<\beta<160$), which means that the distributions are narrower still. Increased

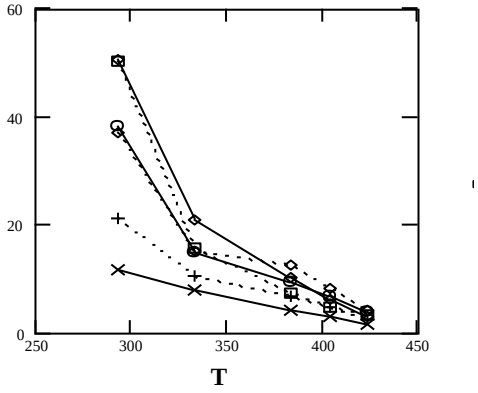

Figure 2b – calculated β parameters with temperature for $1/mH_{dk}$ distributions at various field strengths

temperature caused a reduction in the value of β, and therefore a broadening of the $1/mH_{dk}$ distribution. The characteristic value of the $1/mH_{dk}$ distribution did not change significantly.

DISCUSSION OF RESULTS

Figure 3 shows the form of the $1/mH_{dk}$ and the $1/mS_d$ probability densities. $P(1/mH_{dk})$ is the probability density of the largest values of $1/H_{dk}$ and hence the smallest values of H_{dk} in an infinite number of specimens. The sharp $1/mH_{dk}$ distributions indicate that the minimum activation energies of the ageing process in specimens at a particular E and T are all very similar – they are clustered closely around a characteristic value. It is interesting to note that these very similar minimum activation energies result in broad lifetime distributions. For example, in the DC case, the β values for the $1/mH_{dk}$ distribution ranged between 39 and 160, whilst for the lifetime distributions β ranged from 0.9 to 1.9. Small changes in minimum activation energy have a large effect on the resultant lifetime – particularly at higher temperatures. This is to be expected since lifetime depends exponentially on activation energy. A small variation in the parameters seems physically reasonable, since it implies only a small change in the local environment of each moiety involved in ageing.

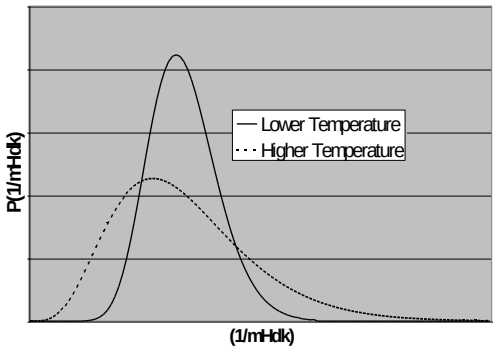

Figure 3 – Weibull extreme value probability density.

At higher temperatures the distribution density of $1/mH_{dk}$ values, $P(1/mH_{dk})$ becomes broader, and this must be due to an increased probability of smaller H_{dk} values in the continuous distribution. The value of $<mH_{dk}>$, which is equal to $1/\alpha$, however, remains constant (until the temperature reaches between 60 and 100°C in the AC case). This increase in probability of activation energies lower than $<mH_{dk}>$ must be balanced by a decrease in the probability of a range of energies above $<mH_{dk}>$. This may be explained if the ageing process is assumed to be one in which rearrangement of polymer segments occurs. The activation energy of this process is an energetic barrier to conformational rearrangement of molecules. Such activation energies form as the polymer solidifies. In the melt, the polymer molecules have very small barriers to conformational rearrangement and the chains can move freely past one another. Barriers are then 'frozen in' as solidification occurs, so that below the glass transition temperature Tg, segmental motions cannot occur at all. Small groups of atoms can vibrate as they are heated, and the range of motions will increase as temperature increases, but no viscous flow is possible.

At temperatures above 60°C to 110°C, i.e. above T_g, the AC results show a whole-scale movement of the $1/mH_{dk}$ and $1/mS_d$ distributions, as $1/\alpha$ (and hence $<mH_{dk}>$ and $<mS_d>$) start to decrease with temperature, as shown for $1/mH_{dk}$ in **fig 2a**. The polymer is no longer constrained to remain globally rigid above these temperatures - the activation energy can therefore begin to decrease, and plastic deformations become possible. The moieties associated with this kind of ageing process are unlikely to be those deep in crystalline parts of the polymer, since these will be subject to the largest activation energies for a process of this type. It has been found, however, that the energy barriers in the DMM model have very similar magnitudes for different materials [2], and this implies that the chemical composition of the polymer does not make an appreciable difference to the activation energies involved in the ageing process. This is unlikely to be the case if it is moieties in the amorphous region that are important, since the morphology of these regions, and hence the barrier distribution to conformational rearrangement, will depend very strongly on the constituent molecule. The same is true of the crystalline regions – the chemical composition of crystalline parts of a polymer will have a large effect on the activation energy associated with freeing chain segments. It therefore seems likely that the breakdown process is characteristic of chain sections confined to the lamella surfaces, which became only partly crystallised as the polymer cooled. These will be the chains which will be most able to move freely once they are initially freed, since they are neither part of a rigid crystalline structure, nor are they likely to be highly tangled as in the amorphous region. The increased freedom of these chain

sections produced during the ageing reaction may eventually be sufficient to remove the constraints on their crystallisation imposed during solidification. Consequently, the sections may crystallise, and low-density regions will therefore be generated in the neighbouring amorphous regions. Such low-density regions have long been associated with breakdown in polymers, through such processes as partial discharge.

In the absence of any stresses, crystallisation in a polymer can only occur between Tg and Tm – the melting point of crystallites, which is dependent on the crystallite size. In fact, crystallisation in PET has been observed to occur above 90°C and below 250°C, W.H. Cobbs and R. L. Burton [10]. It is possible that in a polymer subject to a stress, the chains will be able to crystallise at lower temperatures than normal – i.e. below 90°C for PET. This effect has been observed, J. O. Fernandez and G.M. Swallowe [11] for a macroscopic compressive mechanical stress applied to a PET sample, where crystallisation was observed just above a quoted Tg of 70°C. In this case, a mechanical tension is thought to align polymer chains in such a way as to reduce the energy barrier to crystallisation. A similar reduction in activation energy may occur for an applied electrical stress via local mechanical stress caused by trapped space charge. In this investigation, AC data is available at 60°C and 110°C, but not in-between. Both Tg and the onset of unstressed crystallisation occur between these limits, so it is not possible to tell at what point the ageing energy barrier begins to fall. Nonetheless, the results are consistent with the ageing process being one of crystallisation of lamella surface chains causing a free volume increase in neighbouring amorphous regions.

In the DC case, all the data is above 100°C and hence above Tg. No reduction in the characteristic barrier value is observed. It may be that the ageing process is different in the AC and DC cases, although the constancy of values of the other model parameters between AC and DC is contrary to this. Another possibility is that frequency effects may cause the temperature at which the energy barrier begins to fall to be different between the AC and the DC cases. The much larger values of mH_{dk} found for the DC case and the fact that mS_d is very close to zero suggest that the barrier in the DC case is related to site rearrangements, whereas in the AC case it is related to group rearrangements. It is therefore possible that the difference between AC and DC ageing lies only in the number of polymer monomer units rearranging and not in the process itself. The more localised the individual rearrangements are, the less likely they are to be effected by temperature. Possibly this reflects the fact that in AC fields the whole of the lamella surface may be driven to fluctuate, whereas in DC fields it will be frozen in a specific energy configuration – rearrangement of which requires displacement of the most 'locked in' site.

*Now at Borealis AB, Sweden

CONCLUSION

A distribution of the parameters representing activation energy of the ageing process within the DMM lifetime model has been shown to model experimental lifetime distributions of PET films well. The results imply small differences in the local environments of the moieties involved in the ageing process Very small changes in the minimum activation energy values have a pronounced effect on the resultant lifetimes of polymer specimens. Changes in the distributions of activation energies with field and temperature can be explained by assuming the ageing process to be one whereby polymer segments on lamella surfaces crystallise to create free volume within the polymer.

ACKNOWLEDGEMENT

We thank EPSRC and BICC Cables/Pirelli, for their support, Dr S. Gubanski for the unpublished statistical lifetime data and the University of Leicester for study leave for Professor John Fothergill.

REFERENCES

1. L. A Dissado, G. Mazzanti and, G. C. Montanari 'The Role of Trapped Space Charges in the Electrical Aging of Insulating Materials' IEEE Trans. DEI, **4** No. 5, pp496-506, 1999.
2. G. Mazzanti, G. C. Montanari and L. A Dissado 'A Space-charge Life Model for ac electrical Aging of Polymers' IEEE Trans DEI, **6**, , pp864-875, 1999.
3. T. J. Lewis, P. Llewellyn, M. J. van der Sluijs, J. Freestone, R. N. Hampton, 'A New Model for Electrical Ageing and Breakdown in Dielectrics' 7th DMMA, pp23-26, 1996.
4. J. P. Crine 'A Molecular Model to Evaluate the Impact of Aging on Space Charges in Polymer Dielectrics' IEEE Trans. DEI **4** No. 5, pp487-495, 1997.
5. C. L. Griffiths, S. Betteridge and R. N. Hampton 'Thermoelectric ageing of cable grade XLPE in dry conditions' IEEE ICSD pp279-282, 1997
6. L. A. Dissado, S. J. Urban and P.A. Norman, 'Breakdown Statistics of the Space-charge ageing model for polymeric insulation' CEIDP pp129-132, 1996
7. J. C. Fothergill and L.A. Dissado, 'Electrical degradation and breakdown in polymers'. (P. Peregrinus for IEE, London, :ISBN 0 86341 196 7, 1992)
8. S. Gubanski, private communication.
9. L. A. Dissado, 'The Physics of Electrical Ageing in Semi-crystalline Insulating Polymers', 32nd Symposium on Electrical and Electronic Insulating Materials and Applications in Systems, pp9-16, 2000.
10. W.H. Cobbs and R. L. Burton 'Crystallisation of Polyethylene Terephthalate' Journal of Polymer Science, **10**, No. 3, pp275-290, 1953.
11. J. O. Fernandez and G.M. Swallowe, 'Crystallisation of PET with strain, strain rate and temperature' Journal Mat. Sci., **35**, pp4405-4414, 2000.